Journal of Plant Physiology 215 (2017) 65–72

Contents lists available at ScienceDirect

Journal of Plant Physiology

journal homepage: www.elsevier.com/locate/jplph

FRET-based glucose imaging identifies glucose signalling in response to biotic and abiotic stresses in rice roots

Qingdong Zhu, Li Wang, Qianli Dong, Shu Chang, Kexin Wen, Shenghua Jia, Zhilin Chu, Hanmeng Wang, Ping Gao, Heping Zhao, Shengcheng Han*, Yingdian Wang*

Beijing Key Laboratory of Gene Resource Molecular Development, College of Life Sciences, Beijing Normal University, Beijing, China

ARTICLE INFO

Keywords:
FRET nanosensor
Glucose dynamics
Abiotic stress
Biotic stress
Rice

ABSTRACT

Glucose is the primary energy provider and the most important sugar-signalling molecule, regulating metabolites and modulating gene expression from unicellular yeast to multicellular plants and animals. Therefore, monitoring intracellular glucose levels temporally and spatially in living cells is an essential step for decoding the glucose signalling in response to biotic and abiotic stresses. In this study, the genetically encoded FRET (Förster resonance energy transfer) nanosensors, FLIPglu–2 μΔ13 and FLIPglu–600 μΔ13, were used to measure cytosolic glucose dynamics in rice plants. First, we found that the FRET signal decreased in response to external glucose in a concentration-dependent manner. The glucose concentration at which the cytosolic level corresponded to the $K_{0.5}$ value for FLIPglu–2 μΔ13 was approximately 10.05 μM, and that for FLIPglu–600 μΔ13 was 0.9 mM, respectively. The substrate selectivity of nanosensors for glucose and its analogues is D-Glucose > 2-deoxyglucose > 3-O-methylglucose > L-Glucose. We further showed that the biotic elicitors (flg22 and chitin) and the abiotic elicitors (osmotic stress, salinity and extreme temperature) induce the intracellular glucose increases in the detached root segments of transgenic rice containing FLIPglu–2 μΔ13 in a stimulus-specific manner, but not in FLIPglu–600 μΔ13 transgenic lines. These results demonstrated that FRET nanosensors can be used to detect increases in intracellular glucose within the physiological range of 0.2–20 μM in response to various stimuli in transgenic rice root cells, which indicated that intracellular glucose may act as a potential secondary messenger to connect extracellular stimuli with cellular physiological responses in plants.

1. Introduction

Glucose is the predominant source of carbon energy and the most important sugar-signalling molecule, regulating metabolites and modulating gene expression from unicellular yeast to multicellular plants and animals. Extracellular glucose levels in yeast (*Saccharomyces cerevisiae*) are sensed by the Snf3 and Rgt2 glucose sensors, which are localised on the cell surface. Then, the signal is transduced into the nucleus, activating Rgt1 transcription factor to regulate the transcription expression of glucose transporters via a signalling transduction pathway shared by many kinds of tumour cells (Johnston and Kim, 2005; Gatenby and Gawlinski, 2003). In plants, glucose contributes to a wide range of physiological processes, including germination, seedling development, photosynthesis, carbon and nitrogen metabolism, flowering and seed filling, senescence, and responses to stress and pathogen infection (Chen et al., 2015a; Rolland et al., 2006). In *Arabidopsis thaliana*, it was shown that the regulator of G-protein signalling protein 1 (AtRGS1) as a putative extracellular glucose sensor forms a complex with the heterotrimeric G protein to regulate steady-state levels of transcripts from a small set of sugar-regulated genes in a G-protein-coupled signalling network (Grigston et al., 2008). Despite the essential roles of extracellular glucose as a primary messenger were sensed and utilised in relation to cellular metabolic status and biotic or abiotic stress responses (Lastdrager et al., 2014), the molecular mechanisms of glucose signalling pathways remain elusive in plants and mammals.

The spatial and temporal distribution of glucose in plant cells is a foundation for understanding glucose signalling transduction. Using a non-aqueous fractionation method, about 77%, 14.3%, and 8.7% of glucose was identified in vacuoles, cytosol, and the plastid of potato tubers, respectively (Farré et al., 2001). In the leaves of tobacco, up to

Abbreviations: eCFP, enhanced cyan fluorescent protein; eYFP, enhanced yellow fluorescent protein; FRET, Förster resonance energy transfer; 2-dG, 2-deoxyglucose; 3-OMG, 3-*O*-methylglucose; chitin, chitooctaose octahydrochloride; flg22, flagellin 22

* Corresponding authors.
E-mail addresses: qingdong@mail.bnu.edu.cn (Q. Zhu), 201031200005@mail.bnu.edu.cn (L. Wang), qianlidong@mail.bnu.edu.cn (Q. Dong), clare23@163.com (S. Chang), wkx918@163.com (K. Wen), jiashenghua_37@yahoo.com.cn (S. Jia), zhiriyulin@sina.com (Z. Chu), 201531200012@mail.bnu.edu.cn (H. Wang), gaoping1008@bnu.edu.cn (P. Gao), hpzhao@bnu.edu.cn (H. Zhao), schan@bnu.edu.cn (S. Han), ydwang@bnu.edu.cn (Y. Wang).

http://dx.doi.org/10.1016/j.jplph.2017.05.007
Received 23 January 2017; Received in revised form 16 May 2017; Accepted 16 May 2017
Available online 20 May 2017
0176-1617/

98% of hexose was detected in the vacuole (Heineke et al., 1994). It was further shown that cytosolic glucose concentrations in *Arabidopsis* root cells are < 90 nM in the absence of photosynthesis or an external supply (Deuschle et al., 2006). These results suggested that the vacuole provides a glucose pool involved in glucose metabolism and signalling transduction. Servaites and Geiger (2002) have demonstrated that glucose influx and efflux occur via the inner envelope of plastids, which suggests that some glucose transporters are involved in these processes. SWEET2 as an *Arabidopsis* sugar transporter was identified to be localised to the tonoplast, where it took the role of sequestering glucose in vacuoles and thereby limiting carbon efflux in the cortex and epidermis of roots (Chen et al., 2015a). AtVGT1 (*Arabidopsis thaliana* glucose transporter 1) was localised in the vacuolar membrane, where it was required for the osmotic adjustment and turgor increase during seed germination and flowering (Aluri and Büttner, 2007). SWEET8/RPG1 as a glucose transporter was indicated to be localised to the plasma member, where it was required for exine pattern formation of microspores in *Arabidopsis* (Guan et al., 2008). To date, three classes of eukaryotic sugar transporters, glucose transporters, sodium–glucose symporters, and SWEETs, have been characterised in multicellular organisms (Chen et al., 2015b). Thus, various sugar transporters localised in different membranes contribute to the distribution of glucose in cellular compartments.

Cytosolic glucose can be sensed by hexose kinase (HXK), which is a moonlighting protein involved in glucose metabolism and signalling to regulate growth and development in yeast, mammals, and plants (Dentin et al., 2004; Granot et al., 2013; Moreno et al., 2005). It was proved that *Arabidopsis* HXK1 as an intracellular glucose sensor evokes a response to the changing environment by uncoupling glucose sensing from its phosphorylation with HXK1 mutants lacking catalytic activity, thereby connects nutrient, light and hormone signalling networks for controlling growth and development (Moore et al., 2003). Cho et al. (2006) further demonstrated that HXK1 directly modulates glucose-regulated gene transcription independent of glucose metabolism in *Arabidopsis*, which mainly depends on a glucose signalling complex core with two unconventional, nucleus-specific HXK1 partners, vacuolar H^+-ATPase B1 and the 19S regulatory particle of the proteasome subunit. In addition, OsHXK5, OsHXK6, and OsHXK7 in rice, and NtHXK1 in tobacco, as glucose sensors can complement the *Arabidopsis glucose insensitive2-1* (*gin2-1*) phenotype (Cho et al., 2009; Kim et al., 2013; Kim et al., 2016). Thus, the intracellular glucose and its sensors represent core components involved in decoding the glucose signalling transduction pathway. However, measuring cytosolic glucose levels in living cells remains problematic due to their highly dynamic fluctuation. Using nuclear magnetic resonance spectroscopy and/or gas chromatography mass spectrometry, the distribution of ^{13}C-labelled glucose isotopologs can be used to analyse the labelling patterns by various models for deducing metabolic fluxes (Edwards et al., 1998; Ettenhuber et al., 2005). However, the spatial resolution and subcellular dynamics of the glucose in living cells are limited.

The development of genetically encoded FRET (Förster resonance energy transfer) nanosensors has significantly aided the study of cytosolic glucose dynamics at high spatial and temporal resolution in mammals, yeast, and *Arabidopsis* (Bermejo et al., 2010; Deuschle et al., 2006; Fehr et al., 2003). A set of FRET glucose sensors with different glucose affinities ($K_{0.5}$), covering the low nano- to mid-millimolar range, were produced by the fusion of glucose/galactose-binding protein MglB with a pair of green fluorescent protein variants, an enhanced cyan fluorescent protein (eCFP) and an enhanced yellow fluorescent protein (eYFP) (Deuschle et al., 2005). In *Arabidopsis*, the sensors FLIPglu-170nΔ13, −2 μΔ13, −600 μΔ13, and −3.2mΔ13 were used successfully to monitor steady-state levels of glucose and their changes in response to an external glucose supply in the leaf epidermis or roots (Chaudhuri et al., 2008, 2011; Deuschle et al., 2006). To clarify the physiological roles of glucose as a signalling molecule in rice, it is necessary to use FRET nanosensors to monitor the dynamic level of cytosolic glucose in living cells of rice plants. In this study, we built constructs with FLIPglu–2 μΔ13 and FLIPglu–600 μΔ13 expression driven by UBIQUITIN promoters to express each of these two glucose nanosensors to detect cytosolic glucose changes in detached rice root segments exposed to various biotic and abiotic stresses. Our results indicated that the dynamics of cytosolic glucose detected with FRET nanosensors are within the physiological range in response to different stimuli, suggesting that cytosolic glucose may act as a signalling molecule or a secondary messenger to connect extracellular stimuli with cellular physiological responses in rice plants.

2. Materials and methods

2.1. Rice plant growth

Rice plants (*Oryza sativa* L. spp. *japonica* cv. Zhonghua11) were planted in a growth chamber and in fields (from May to October, annually) at Beijing Normal University (Beijing, China). Transgenic rice plants were regenerated from the transformed calli on selection media containing 50 mg/L hygromycin and 250 mg/L cefotaxime after the calli had been incubated with *Agrobacterium tumefaciens GV3101* containing FLIPglu–2 μΔ13 or FLIPglu–600 μΔ13. To produce homozygous transgenic rice lines (T_3), transgenic plants were selected by 3:1 separation in the growth chamber and grown in the field for several generations. The transgenic lines were grown in the chamber under a 14-h light (24 °C)/10-h dark (20 °C) photoperiod and relative humidity of 85%. After culturing for approximately 10 days in Yoshida's culture medium (Yoshida et al., 1976) that was replaced each day, the seedlings were ready for glucose imaging.

2.2. Chemical reagents

All chemicals except those mentioned elsewhere were purchased from Sigma-Aldrich (St. Louis MO, USA). Flg22 was dissolved in dimethylsulfoxide to make a 1 mM stock solution. Chitooctaose (Chitin) purchased from Qingdao BZ Oligo Biotech Co. Ltd (Qingdao, China) was dissolved in water to make a 1 mM stock solution and kept at −20 °C. Before use, the flg22 and Chitin stock solution were diluted in Yoshida's culture solution to 100 nM. Sorbitol and NaCl were dissolved in Yoshida's culture solution to 250 or 300 mM, respectively. D-glucose (D-Glu), 2-deoxyglucose (2-dG), 3-O-methylglucose (3-OMG), and L-Glucose (L-Glu) were respectively dissolved in water to make 1 M stock solutions, which were diluted in Yoshida's culture solution to the appropriate concentrations prior to use.

2.3. Vector constructs for expression in rice

The plasmids, *pFLIPglu–2 μΔ13* and *pFLIPglu–600 μΔ13,* were purchased from Addgene (http://www.addgene.org/, plasmid ID 12990 and 12991). The DNA fragments of *FLIPglu–2 μΔ13* and *FLIPglu–600 μΔ13* were amplified and ligated into pTCK303 (Wang et al., 2004) via the restriction enzyme sites Kpn I/Spe I flanking the cassette. The plasmids were introduced into *Agrobacterium tumefaciens GV3101* and prepared for rice transformation. The primer sequence of *FLIPglu* used for the PCR amplification is provided in Table S1, and the construct maps for *FLIPglu–2 μΔ13* and *FLIPglu–600 μΔ13* are presented in Supplementary Fig. S1. The vectors were verified by DNA sequencing.

2.4. Expression analyses of FLIP glucose nanosensors in transgenic rice

Total RNA was prepared from one-week-old transgenic seedlings using TRIzol® reagent (Life Technologies, USA) and purified using a PureLink® RNA Mini Kit (Invitrogen, USA) combined with a PureLink® DNase Kit (Invitrogen), in accordance with the manufacturers' protocols. RNA concentration and quality were measured using a NanoVue

spectrophotometer (GE Healthcare, USA). Approximately 2 μg total RNA was used for the synthesis of cDNA using the TransScript One-Step gDNA Removal and cDNA Synthesis Kit in accordance with the manufacturer's manual (TransGen, China). The cDNA was used for each RT-PCR reaction with gene-specific primers, and the rice *Actin* gene (Os03g0718100) was used as an internal control. The number of PCR cycles was calibrated for each pair of primers: 28 cycles for *FLIPglu–2 μΔ13* and *FLIPglu–600 μΔ13* and 26 cycles for *Actin*. The primer sequence used for the RT-PCR is provided in Table S1.

2.5. Protein gel blot analysis

The transgenic rice seedlings were frozen in liquid nitrogen and ground using a mortar. The samples were incubated on ice for 30 min in lysis buffer containing 50 mM Tris-HCl, pH 8.0, 150 mM NaCl, 10% glycerol, 0.1% Nonidet P-40, 0.1% Triton X-100, 50 mM DTT, and the appropriate protease inhibitor cocktail (Roche, Switzerland), and then centrifuged at 14,000*g*, 4 °C, for 10 min. Supernatants were quantified using BCA Protein Assay Kits in accordance with the manufacturer's manual (GenStar, USA). Protein extracts (20 μg per lane) were resolved on 12% sodium dodecyl sulphate-polyacrylamide gels and electro-blotted onto Bio-Rad Immun-Blot polyvinylidene fluoride (PVDF) membranes (Bio-Rad, USA). After transfer, PVDF membranes were blocked in Tris-buffered saline-Tween 20 (TBST; containing 10 mM Tris–HCl, pH 8.0, 150 mM NaCl, 0.05% Tween 20) containing 5% bovine serum albumin (Sigma-Aldrich) for 1 h at room temperature and incubated with the primary antibody of mouse green fluorescent protein (Sigma-Aldrich, dilution 1:1000) overnight at 4 °C. Membranes were washed three times (10 min) in TBST and incubated with the secondary antibody of anti-mouse immunoglobulin G (Sigma-Aldrich, dilution 1:2000) for 30 min. Subsequently, the membranes were washed three times (10 min) in TBST. Alkaline phosphatase activity was examined by Chemiluminescent Substrate (Roche) in accordance with the manufacturer's protocol.

2.6. In vivo glucose imaging

Cytosolic glucose levels were measured using FRET nanosensors by a modified version of a previously described method (Chaudhuri et al., 2008, 2011; Deuschle et al., 2006). To reduce endogenous sugar levels, rice seedlings were cultured in Yoshida's solution at room temperature for 24 h in darkness before measurement. Then, the fragments of young fibrous roots of 10-day-old seedlings were separated and immobilised on coverslips (Fisher Scientific, USA) using low-melting-point agarose (Amresco, USA), and the parts of the root were exposed. The coverslips were put in an Attofluor® Cell Chamber (Invitrogen) to form a perfusion chamber (Supplementary Fig. S4). The samples were incubated with 300 μl Yoshida's culture solution for 15 min prior to imaging. Measurements were carried out using a flaring pipette to quickly remove the incubated solution, and then a new 300 μl Yoshida's culture solution plus different chemicals was added. D-Glu, 2-dG, 3-OMG, L-Glu, flg22, chitin, sorbitol, and NaCl were dissolved in Yoshida's culture solution at the appropriate concentrations, respectively. Prior to treatment with high or low temperature stress, the Yoshida's culture solutions were incubated in 50 °C water bath as the high-temperature stresser or kept in ice water (0 °C) as the low-temperature stressor, and 300 μl Yoshida's culture solution was added to the perfusion chamber for continual imaging.

FRET imaging was performed with an inverted fluorescence microscope (Axio Observer A1; Zeiss, Germany) using an iXon3 EMCCD camera (Oxford Instruments, UK), Bright Line filter sets (Semrock Inc., USA), a × 40 oil objective (numerical aperture = 1.30, Zeiss), and Metafluor 7.0 software (Molecular Devices, UK). Excitation was provided by a Lambda DG4 fluorescent light source (Sutter Instruments, USA). Raw images (F_{CFP}, F_{YFP}, and F_{raw}) were collected every 5 s using the above-mentioned imaging system equipped with an Optosplit II Image Splitter (Cairn Research Limited, UK) and the following combination of Semorock Bright Line filter sets that constitute three equivalent filters: CFP ($428.9 \pm 5.5_{Ex}/465 \pm 32_{Em}$), YFP ($502.6 \pm 11.2_{Ex}/549 \pm 21_{Em}$), and $FRET_{raw}$ ($428.9 \pm 5.5_{Ex}/549 \pm 21_{Em}$). All experiments were carried out at room temperature.

2.7. Glucose imaging data analysis

Three-channel-corrected FRET was calculated and analysed as described previously (Ma et al., 2015). Briefly, the FRET signal was first calculated using the following formula: $FRET_c = F_{raw} - F_d/D_d * F_{CFP} - F_a/D_a * F_{YFP}$, where $FRET_c$ represents the corrected total amount of energy transfer, F_d/D_d represents the measured bleed-through of CFP into the FRET filter (0.826), and F_a/D_a is the measured bleed-through of YFP through the FRET filter (0.048). Then, $FRET_c$ values were normalised against donor fluorescence (F_{CFP}) to generate the N-FRET (normalised FRET) signal to reduce variations caused by differences in expression levels. To eliminate instrument-dependent factors, the apparent FRET efficiency (Eapp) was calculated using the following formula: Eapp = N-FRET/(N-FRET + G), where G (4.59) is a system-dependent factor. It is obtained using a partial YFP photo-bleaching method: $G = (FRET_c - FRET_c^{post})/(F_{CFP}^{post} - F_{CFP})$, where $FRET_c^{post}$ and F_{CFP}^{post} are corresponding $FRET_c$ and F_{CFP} values after partial photo-bleaching of YFP. In this study, Eapp is compared with resting Eapp ($Eapp_{rest}$) levels and denoted as $Eapp/Eapp_{rest}$, where $Eapp_{rest}$ is the resting Eapp before the application of various reagents. The maximum changes in Eapp (ΔEapp) were compared with resting Eapp ($Eapp_{rest}$) levels, and they are denoted as $\Delta Eapp/Eapp_{rest}$, in which $\Delta Eapp = Eapp - Eapp_{rest}$. The relative maximum Eapp change ($\Delta Eapp/Eapp_{rest}$) at various glucose concentrations and for other reagents was plotted and fitted to a single-site binding isotherm to determine the *in vivo* $K_{0.5}$, that is, the external glucose concentration at which the cytosolic levels correspond to the $K_{0.5}$ of the respective sensor. All fluorescence images were collected and briefly processed using MetaFluor software (Molecular Devices), and then the resulting data were further analysed using Matlab R2012b software and plotted using Prism 5 software.

2.8. Statistical analyses

The average FRET measurement for each data point represents three independent experiments and a total of 20 individual root cells. Analysis of statistical significance was performed using the unpaired Student's *t*-test with GraphPad Prism 5 software. $P < 0.05$ was considered to indicate statistical significance. Data are presented as the mean ± SD.

3. Results

3.1. Expression of FLIP glucose nanosensors in rice plants

To monitor cytosolic glucose levels in rice, we separately developed transgenic rice overexpressing the nanosensors FLIPglu–2 μΔ13 and FLIPglu–600 μΔ13 under the control of the ubiquitin promoter in a binary vector, pTCK303 (Wang et al., 2004) (Supplementary Fig. S1). The expressions of nanosensors up to the T_3 homozygous generation were detected by reverse transcription polymerase chain reaction (RT-PCR) at the RNA level and by Western blot analysis at the protein level. It was found that the nanosensors were expressed consistently in the whole plant and among different tissues, such as young embryos, roots, leaves, and stems (Supplementary Fig. S2). In addition, the root and shoot growth for 10-day rice seedlings were compared between the transgenic rice lines expressing *FLIPglu–2 μΔ13* and *FLIPglu–600 μΔ13* and the wild type (WT), respectively. It was found that the heterologous expression of the nanosensors FLIPglu–2 μΔ13 and FLIPglu–600 μΔ13 had no effects on the growth of transgenic rice as compared with WT (Supplementary Fig. S3), which suggested that these transgenic plants

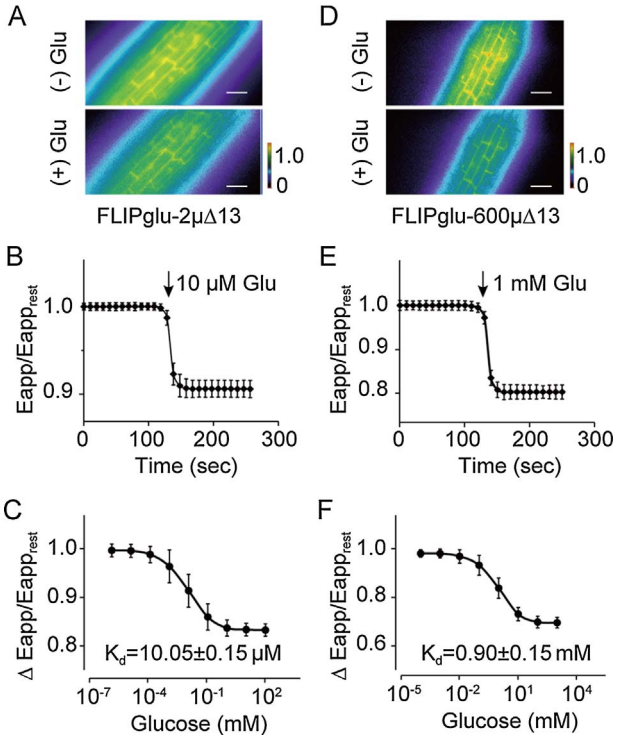

Fig 1. Glucose-induced FRET changes in the cytosol of fibrous roots of 10-day-old transgenic rice plants. A, FRET signal image of the tip of a rice root expressing FLIPglu–2 μΔ13 before the application of glucose (top) and the response to glucose perfusion (bottom). The intensity of the FRET signal is indicated by a pseudo-colour bar (bottom right). Scale bar, 20 μm. B, Time course of glucose-induced FRET signal change in the detached root segments of FLIPglu–2 μΔ13 transgenic rice. Twenty individual cells are shown. The arrow indicates the perfusion time of 10 μM glucose (Glu). C, The average change of negative relative maximum Eapp (ΔEapp/Eapp$_{rest}$) plotted as a function of the applied glucose concentration in the experiments performed as in A (n = 20 cells). Data were fitted to the Hill equation to get a K_d of 10.05 ± 0.15 μM, and the Hill coefficient was about 1. D, FRET signal image of the tip of a rice root expressing FLIPglu–600 μΔ13 before the application of glucose (top) and the response to glucose perfusion (bottom). E, Time course of glucose-induced FRET signal change in the detached root segments of FLIPglu–600 μΔ13 transgenic rice. Twenty individual cells are shown. The arrow indicates the perfusion time of 1 mM glucose (Glu). F, The average change of negative relative maximum Eapp (ΔEapp/Eapp$_{rest}$) plotted as a function of the applied glucose concentration in the experiments performed as in A (n = 20 cells). Data were fitted to the Hill equation to get a K_d of 0.90 ± 0.15 mM, and the Hill coefficient was about 1. All error bars denote SEM for at least three independent experiments, each of which included six to eight single cells.

were suitable for subsequent glucose measurement experiments.

3.2. High-resolution analysis of cytosolic glucose dynamics in rice roots

A previous study showed that rice leaf wax prevents the permeation of coelenterazine to block aequorin luminescence (Zhang et al., 2015). Therefore, we speculated that leaf wax would prevent fluctuations in the external supply of glucose into cells, and we used the fibrous root segments of transgenic rice to measure glucose dynamics in response to different stresses. First, we observed YFP fluorescence, CFP fluorescence, and FRET signals from the transgenic plants expressing *FLIPglu–2 μΔ13* and *FLIPglu–600 μΔ13* (Supplementary Fig. S5). When the detached root segments were immersed in Yoshida's solution, we detected the increased CFP fluorescence and the decreased YFP fluorescence after adding 10 μM glucose for FLIPglu–2 μΔ13 transgenic rice and 1 mM glucose for FLIPglu–600 μΔ13 transgenic rice, which produced an intense FRET signal (Supplementary Fig. S1C; Supplementary Fig. S6), suggesting that extracellular glucose induced the increase of cytosolic glucose (Fig. 1A and B, D and E). This observation was consistent with previous studies (Chaudhuri et al., 2008, 2011; Deuschle et al., 2006). The average changes of negative relative maximal FRET

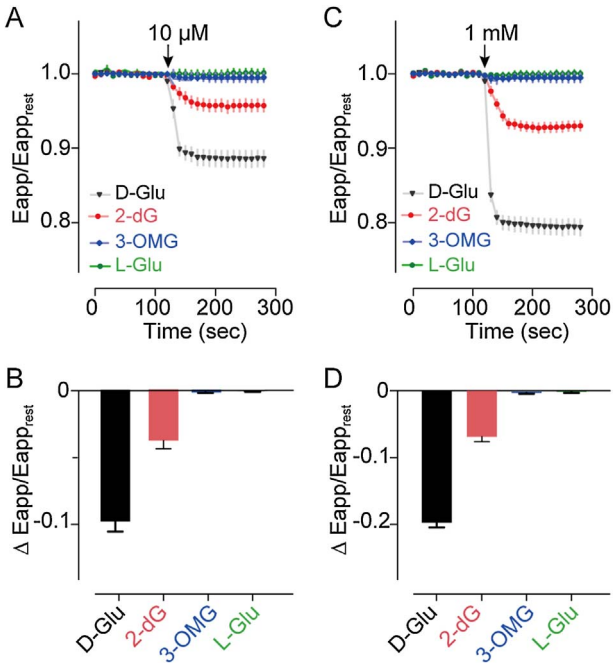

Fig. 2. Selectivity of FRET nanosensor for glucose (D-Glu) over its structural analogues 2-deoxyglucose (2-dG), 3-O-methylglucose (3-OMG), and L-glucose (L-Glu). A and C, Time course of FRET signal changes in response to D-Glu and its analogues in the detached root segments of FLIPglu–2 μΔ13 transgenic rice (A) and FLIPglu–600 μΔ13 transgenic rice (C), respectively. Other conditions were the same as given in Fig. 1. The arrow indicates the perfusion times of 10 μM glucose and its analogues for FLIPglu–2 μΔ13 transgenic rice or 1 mM glucose and its analogues for FLIPglu–600 μΔ13 transgenic rice. B and D, The average change of negative relative maximum Eapp (ΔEapp/Eapp$_{rest}$) in response to 10 μM D-Glu and its analogues for FLIPglu–2 μΔ13 transgenic rice (B) or 1 mM D-Glu and its analogues for FLIPglu–600 μΔ13 transgenic rice (D). All error bars denote the SEM for at least three independent experiments, each of which included six to eight single cells.

signal (ΔEapp/Eapp$_{rest}$; Eapp, the apparent FRET efficiency) at various glucose concentrations were plotted and fitted to a single-site binding isotherm to determine the apparent in vivo $K_{0.5}$. The external glucose concentrations at which the cytosolic level corresponded with the $K_{0.5}$ of FLIPglu–2 μΔ13 and FLIPglu–600 μΔ13 were approximately 10.05 μM with a ΔEapp/Eapp$_{rest}$ of 0.106, and 0.9 mM with a ΔEapp/Eapp$_{rest}$ of 0.196, respectively (Fig. 1C and F). It is possible that extracellular glucose provides a direct driving force for glucose influx, which could be mediated by SWEET transporters across the plasma membrane (Chen et al., 2010). We further measured glucose dynamics for the different regions of transgenic rice fibrous roots in response to extracellular glucose treatment and found no apparent differences among fibrous root regions (Supplementary Fig. S7).

3.3. Comparison of substrate selectivity for two FRET nanosensors

To determine substrate specificity of gluocose nanosensors, we compared the FRET signal change in response to glucose (D-glucose, D-Glu) and several analogues, 2-deoxyglucose (2-dG), 3-O-methylglucose (3-OMG), and L-glucose (L-Glu), in FLIPglu–2 μΔ13 and FLIPglu–600 μΔ13 transgenic plants. As shown in Fig. 2, the rank order of ΔEapp/Eapp$_{rest}$ was D-Glu > 2-dG > 3-OMG > L-Glu upon perfusion of these glucose analogues at the concentrations of 10 μM for FLIPglu–2 μΔ13 transgenic rice (Fig. 2A and B) and 1 mM for FLIPglu–600 μΔ13 transgenic rice (Fig. 2C and D), respectively. L-Glu is not a natural product and cannot be recognised by the glucose/galactose-binding protein. There were no changes in the intensity of CFP fluorescence and YFP fluorescence after adding 10 μM L-Glu for FLIPglu–2 μΔ13 transgenic rice and 1 mM L-Glu for FLIPglu–600 μΔ13 transgenic rice (Supplementary Fig. S8). Therefore, L-Glu cannot induce a FRET signal change, although it can enter solely by diffusion (Lin

et al., 1984). A previous study showed that 2-dG and 3-OMG were taken up by high-affinity glucose transport systems (Bessell and Thomas, 1973). We found that 2-dG induced a delayed cytoplasmic glucose spike in detached rice root segments and led to a 30% decrease in Eapp as the FRET signal changed upon glucose perfusion at the same concentration, but 3-OMG showed no effects or only marginal effects on FRET signal changes. These results were consistent with a previous study showing that 2-dG and 3-OMG cannot induce a significant decrease in the FRET signal at physiological concentrations for the FLIPglu–600 μ construct (Fehr et al., 2003). Thus, FLIPglu–2 μΔ13 and FLIPglu–600 μΔ13 displayed high substrate selectivity and were suitable for monitoring glucose dynamics in rice root cells.

3.4. Biotic elicitors flg22 and chitin induced cytosolic glucose increase in the detached root segments of FLIPglu–2 μΔ13 transgenic rice

Plants have developed complex signalling networks to regulate their growth and development in response to various abiotic and biotic environmental changes. A previous study showed that pathogens may hijack host sugar efflux systems to acquire glucose from their hosts for growth (Chen et al., 2010). However, less is known about the response of cytosolic glucose dynamics to pathogen infection in living cells. Here, we detected the changes of FRET signal in response to the biotic elicitors flg22 (flagellin 22) and chitin (chitooctaose octahydrochloride) in the detached root segments of 10-day-old plants expressing *FLIPglu–2 μΔ13* and *FLIPglu–600 μΔ13*. After separately sensing the stimuli of 100 nM flg22 and 100 nM chitin, a rapid negative change of FRET signal occurred in the root cells of FLIPglu–2 μΔ13 transgenic plants, and the $\Delta Eapp/Eapp_{rest}$ was 0.03 for flg22 and 0.02 for chitin (Fig. 3A and B). Increased CFP fluorescence and decreased YFP fluorescence were detected after adding 100 nM flg22 and 100 nM chitin (Supplementary Fig. S9). The flg22 and chitin concentrations at which the cytosolic glucose level corresponded with the $K_{0.5}$ value were approximately 103 nM for flg22 and 119 nM for chitin (Fig. 3C and D). These results demonstrate that biotic elicitors induce increases in cytosolic glucose levels in plants. We also treated the detached root segments of 10-day-old plants expressing *FLIPglu–2 μΔ13* with Yoshida's Culture Solution as a control experiment and found no apparent changes in the FRET signal (Supplementary Fig. S10). Furthermore, no responses occurred under the same stimuli for FLIPglu–600 μΔ13 transgenic rice (Supplementary Fig. S11), suggesting that the cytosolic glucose accumulation fluctuated within the physiological range of ~0.2–20 μM, beyond the range of FLIPglu–600 μΔ13 (between 60 and 6000 μM), under the tested conditions.

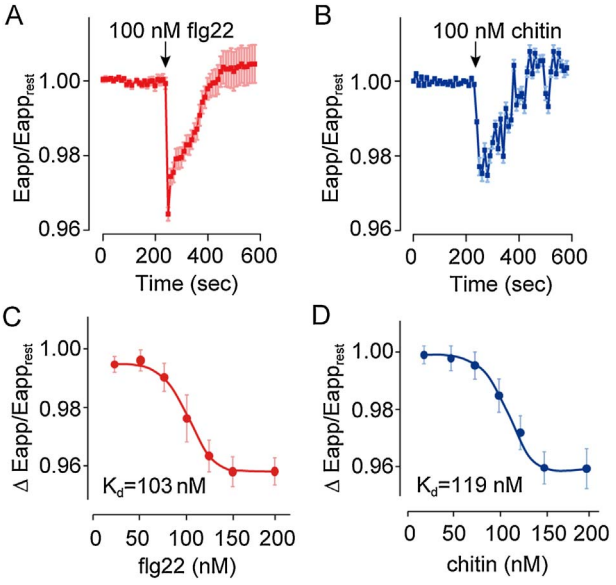

Fig. 3. Biotic stresses induced FRET changes in the cytosol of fibrous roots of FLIPglu-2 μΔ13 transgenic plants. A and B, Time course of FRET signal changes in response to 100 nM flg22 (A) or 100 nM chitin (B) in the detached root segments of FLIPglu–2 μΔ13 transgenic rice. The arrow indicates the perfusion time of flg22 and chitin. C and D, The average change of negative relative maximum Eapp ($\Delta Eapp/Eapp_{rest}$) plotted as a function of the applied flg22 (C) or chitin (D) under the different concentrations (n = 20 cells). Data were fitted to the Hill equation to get a K_d of approximately 103 nM for flg22 and 119 nM for chitin, and the Hill coefficient was about 2. All error bars denote SEM for at least three independent experiments, each of which included six to eight single cells.

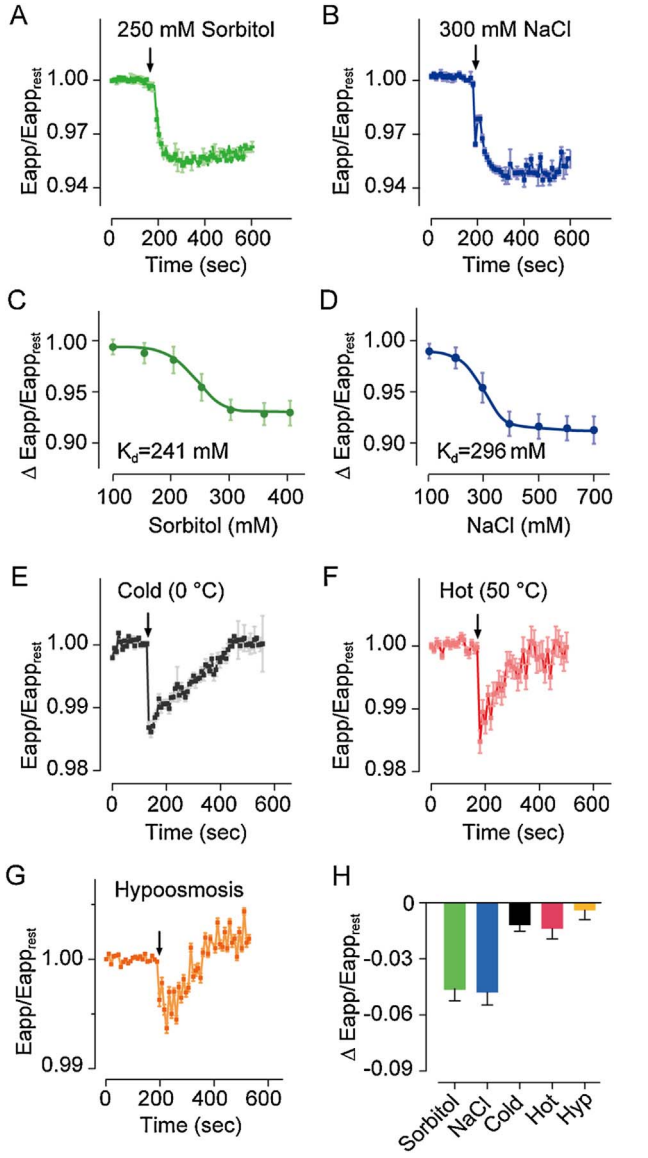

Fig. 4. Abiotic stresses induced FRET changes in the cytosol of fibrous roots of FLIPglu-2 μΔ13 transgenic plants. A, B, E, F, and G, Time course of FRET signal changes in response to 250 mM sorbitol (A), 300 mM NaCl (B), low temperature of 0 °C (E), high temperature of 50 °C (F), and hypoosmosis (G) in the detached root segments of FLIPglu–2 μΔ13 transgenic rice, respectively. Other conditions were the same as given in Fig. 1. The arrow indicates treatment time of different abiotic stresses. C and D, The average change of negative relative maximum Eapp ($\Delta Eapp/Eapp_{rest}$) plotted as a function of the applied sorbitol (C) or NaCl (D) under the different concentrations (n = 20 cells). Data were fitted to the Hill equation for getting a K_d of approximately 241 mM for sorbitol and 296 mM for NaCl, and the Hill coefficient was about 2. H, The average change of relative maximum Eapp ($\Delta Eapp/Eapp_{rest}$) in response to different abiotic stresses. All error bars denote SEM for at least three independent experiments, each of which included six to eight single cells.

3.5. Abiotic stresses induced increased cytosolic glucose in the detached root segments of FLIPglu–2 μΔ13 transgenic rice

Temperature, osmotic stress, and salinity are the three main abiotic stresses affecting plant growth, development, and seed production. When the detached root segments of a 10-day-old plant expressing *FLIPglu–2 μΔ13* were treated with 250 mM sorbitol, the FRET signal decreased rapidly and reached a steady state after ~1 min, the ΔEapp/$Eapp_{rest}$ was 0.046 (Fig. 4A and H), and the sorbitol concentration at which the cytosolic glucose level corresponded to the $K_{0.5}$ was approximately 241 mM (Fig. 4C). The salinity stress associated with 300 mM NaCl treatment also induced a rapid intracellular glucose increase and maintained an ΔEapp/$Eapp_{rest}$ of 0.053 during the measurement period for FLIPglu–2 μΔ13 transgenic rice (Fig. 4 B and 4H). The NaCl concentration at which the cytosolic glucose levels corresponded to the $K_{0.5}$ was approximately 296 mM (Fig. 4D). It was interesting to note that a glucose spike in the cytoplasm occurred within 30 s, with a subsequent occurrence of glucose fluctuations, after the induction by 300 mM NaCl treatment (Fig. 4B). This differs from high-sorbitol-concentration osmotic stress and indicates that different glucose signalling pathways triggered by salinity stress are involved in rice root cells. We also investigated the change in cytosolic glucose in response to hypoosmotic stress for FLIPglu–2 μΔ13 transgenic rice roots and found that the decreased FRET signal in response to hypoosmosis was detectable within 60 s and reached an average change in negative relative maximum ΔEapp/$Eapp_{rest}$ of 0.004 (Fig. 4G and H). These results show that osmotic-related stresses can induce an increase in cytosolic glucose in plant cells.

To investigate whether cytosolic glucose levels change in response to temperature stressors in rice, we measured FRET changes under low (0 °C) and high (50 °C) temperatures in the detached root segments of FLIPglu–2 μΔ13 transgenic rice. The FRET signal decreases in response to these treatments were detected in less than 10 s, with the responses reaching a ΔEapp/$Eapp_{rest}$ of ~0.012 before gradually returning to baseline levels (Fig. 4E, F and H). We found that the curves of FRET signal changes were similar between the low- and high-temperature treatments, but the cytosolic glucose dynamics changed more drastically under the high-temperature treatment. The intensity changes in CFP and YFP that produced the FRET signals after treatment with different abiotic stressors in the detached roots of FLIPglu–2 μΔ13 transgenic rice are shown in Supplementary Fig. S12. We did not note any responses with the treatment of abiotic stresses in FLIPglu–600 μΔ13 transgenic rice (Supplementary Fig. S13). These results show that the glucose nanosensor is an effective tool for obtaining physiological insight into the changes in free cytosolic glucose levels in response to various stimuli in rice plants.

4. Discussion

Plant growth and development are dependent on the coordinated roles of production, distribution, and allocation of assimilates. The partitioning of photoassimilates among different plant tissues is determined by the stage of growth and development and is affected by biotic and abiotic factors such as pathogens, salinity, drought, and extreme temperature (Biemelt and Sonnewald, 2006; Chen et al., 2015b; Shah and Paulsen, 2003; Turhan and Ergin, 2012). Substantial evidence has shown that exogenous glucose reprograms transcription networks via various signal transduction pathways to coordinate nutrient status and growth and development in plants (Lastdrager et al., 2014; Smeekens and Hellmann, 2014; Xiong et al., 2013). In addition, the homeostasis of endogenous glucose is determined by glucose transported into or out of the cytosol, phosphorylation metabolism, and photosynthesis. Therefore, it is essential to detect temporal glucose levels in living cells at a cellular or even subcellular resolution in order to characterise glucose signalling pathways. In this study, we used genetically encoded FRET nanosensors to monitor the dynamics of cytosolic glucose in detached rice root segments and found that extracellular glucose, biotic stress-related elicitors flg22, and chitin and abiotic stressors (such as osmotic stress and extreme temperature) induced increases in cytosolic glucose in rice root cells. This suggested that cytosolic glucose may act as a secondary messenger to connect extracellular or intracellular stimuli with cellular physiological responses in rice growth and development.

According to the method described by Deuschle et al. (2006), we reconstructed FLIPglu–2 μΔ13 (K_d ~2 μM; range ~0.2–20 μM) and FLIPglu–600 μΔ13 (K_d ~600 μM; range ~60–6000 μM) to express these two glucose nanosensors in rice. Using these transgenic rice lines, glucose dynamics were first detected in response to external glucose at various concentrations in detached rice root segments. First, we found that the nanosensors FLIPglu–2 μΔ13 and FLIPglu–600 μΔ13 expressed consistently in the different tissues, such as young embryos, roots, leaves, and stems, have no effects on the growth of transgenic rice as compared with WT. We also found no apparent differences in glucose dynamics for the different root regions, such as maturation zone, meristematic zone, and elongation zone, in response to external glucose at the same concentration, suggesting that detached root segments are a suitable system for monitoring the change of internal glucose in rice. In this study, we found that the levels of cytosolic glucose corresponding to their $K_{0.5}$ values were approximately 10.05 and 900 μM for FLIPglu–2 μΔ13 and FLIPglu–600 μΔ13 in rice root cells, respectively. These levels are greater than the $K_{0.5}$ of approximately ~4 μM for FLIPglu–2 μΔ13, and consistent with the $K_{0.5}$ of 0.8–1 mM for FLIPglu–600 μΔ13, in *Arabidopsis* root cells (Chaudhuri et al., 2011). Moreover, the concentrations of extracellular glucose applied to reach the corresponding K_d value for FLIPglu–2 μΔ13 differed between rice and *Arabidopsis,* which may be attributed to morphological differences in their root architecture. For example, the cortex of rice roots is formed by five cell layers (Coudert et al., 2010), which could limit the diffusion of low-concentration exogenous glucose into root cells. On the other hand, the members of glucose transporters localised in the plasma membrane, such as multiple members of the SWEET family, differ among various plant species, and their affinities to glucose have been found to mediate the influx and efflux of sugar molecules (Chen et al., 2010). Therefore, the levels of cytosolic glucose corresponding to the extracellular glucose treatments vary widely among plant species, which may explain their differences in glucose signal generation.

Glucose nanosensors FLIPglu–2 μΔ13 and FLIPglu–600 μΔ13 were developed by flanking the mutant forms of glucose/galactose-binding protein MglB from *E. coli* fused to ECFP and EYFP via six amino acid linkers at the N and C termini, and the glucose nanosensers displayed a higher substrate selectivity for glucose and galactose than other hexoses and allowed specific monitoring of reversible glucose dynamics in the physiological concentrations range (Fehr et al., 2003; Deuschle et al., 2005; 2006). Fehr et al. (2003) showed that 2-dG and 3-OMG at 1 and 10 mM concentrations cannot induce a significant decrease in ratio for FLIPglu–600 μ in vitro and in vivo, except at non-physiological levels of 100 mM. Ratio changes for DG and 3-O-methylglucose were 50 and 30% of the ratio change at saturating glucose concentrations, respectively. In this study, we compared the FRET signal change of glucose nanosensor between binding D-Glu and its structure analogues, 2-dG, 3-OMG, and L-Glu, in FLIPglu–2 μΔ13 or FLIPglu–600 μΔ13 transgenic rice and found that 2-dG induced a 30% decrease, 3-OMG showed no effects or only marginal effects, and L-Glu exhibited no effects on FRET signal changes at the same concentration with D-Glu. Therefore, the substrate selectivity of nanosensors for glucose and its analogues was D-Glu > 2-dG > 3-OMG > L-Glu. We also found that physiological concentrations of fructose and maltose cannot induce a significant decrease in FRET ratio in FLIPglu–2 μΔ13 or FLIPglu–600 μΔ13 transgenic rice plants (data not shown), which is in agreement with previous studies (Deuschle et al., 2005; 2006). These results suggested that FLIPglu–2 μΔ13 and FLIPglu–600 μΔ13 can be used to specifically monitor the change of cytosolic glucose in both plant and animal cells.

In plant-microbe interactions, plants release metabolites, including sugars, into the surrounding environment, potentially contributing to the growth of microorganisms or to limiting the availability of nutrients to pathogens; similarly, microorganisms can also secrete small molecules to promote plant growth or to obtain nutrients and suppress host immunity (Bais et al., 2006). Recent studies have shown that the expression levels of various sugar transporter genes (*SWEETs*) in rice, which were induced by bacterial symbionts and fungal and bacterial pathogens, were achieved by the direct binding of bacterial transcription activator-like effectors to the SWEET promoter, indicating that the sugar efflux function of SWEET transporters is probably targeted by pathogens and symbionts for nutritional gain (Chen et al., 2010; Zhou et al., 2015). It was also demonstrated that *SWEET2*, a putative sugar transporter that is highly expressed in *Arabidopsis* roots, modulates sugar secretion to prevent the loss of sugar from root tissue to the rhizosphere and contributes to resistance to *Pythium* (Chen et al., 2015a). These results imply that the levels of cytosolic glucose and its fluctuations in plant cells can be affected by environmental stress and are determined by the transport of sugar transporters. Thus, it would be very interesting to determine whether cytosolic glucose acts as a secondary messenger in response to pathogen infection. In the present study, we found that flg22 and chitin as pathogen elicitors can separately induce a transient increase in cytosolic glucose in a concentration-dependent manner in FLIPglu–2 μΔ13 transgenic rice roots. Consequently, we inferred that cytosolic glucose may act as a potential secondary messenger involved in the responses to biotic stress in plants, in a manner similar to cytosolic calcium, reactive oxygen species, and inositol 1,4,5-trisphosphate (Dodd et al., 2010; Steinhorst and Kudla, 2014).

Plants encounter various abiotic stressors during growth and development, such as drought, salinity, and extreme temperatures. In response to various stress stimuli, plants develop complex signalling networks to redistribute water and soluble sugars among different tissues and organs (Gargallo-Garriga et al., 2014). It would be highly advantageous to have high-resolution spatial and temporal information to directly monitor the levels of cytosolic glucose and its fluctuations in plant cells in response to various environmental stimuli. In the present study, we measured glucose dynamics in response to different abiotic stressors, such as hyperosmosis, hypoosmosis, salinity, and high or low temperatures, and found that all of these abiotic factors can increase the concentrations of cytosolic glucose to various extents in rice root cells. More interestingly, the results of this study indicated that hyperosmotic and salt stressors triggered a rapid but lasting increase in cytosolic glucose levels and that hyperosmotic stress (as the first phase of salt stress) contributes to the dynamics of cytosolic glucose (Shavrukov, 2013). Similar to the dynamics of cytosolic glucose in response to the pathogen elicitor flg22 and chitin in rice, we also detected transient and rapid increases in cytosolic glucose under extreme temperatures and hypoosmotic stress. These results indicated that cytosolic glucose may act as a secondary signalling molecule to regulate sugar metabolism and other physiological processes in plants. However, many challenges remain in the study of glucose signal transduction in response to environmental stress, including the identification of additional glucose sensors, the characterisation of regulatory networks associated with different stimuli, and the crosstalk between glucose signalling and other signalling pathways, such as phytohormones and calcium signal transduction. Therefore, expanding our understanding of the roles of environmental and developmental cues throughout the plant life cycle requires further research on the components and underlying mechanisms of glucose signalling networks.

5. Conclusions

Glucose is not only a primary energy provider, but also the most important sugar signalling molecule regulating the expression of genes associated with plant growth and development. Using the genetically encoded FRET-based nanosensors FLIPglu–2 μΔ13 and FLIPglu–600 μΔ13, we investigated the dynamics of cytosolic glucose in detached rice root segments treated with various biotic and abiotic stimuli. We found that these stimuli can increase cytosolic glucose levels in the physiological range of 0.2–20.0 μM in the roots of FLIPglu–2 μΔ13 transgenic rice. These results suggest that cytosolic glucose may act as a secondary signalling molecule that connects extracellular stimuli with cellular physiological responses in plants.

Funding

This work was supported by the National Key Basic Research Program of China (973 Program, 2013CB126902) and the National Natural Science Foundation of China (No. 31370307 and 31070250).

Acknowledgements

The authors acknowledge Dr. Youjun Wang (Beijing Normal University) for his technical assistance in the measurement of FRET signals. The authors have declared no conflicts of interest.

Appendix A. Supplementary data

Supplementary data associated with this article can be found, in the online version, at http://dx.doi.org/10.1016/j.jplph.2017.05.007.

References

Aluri, S., Büttner, M., 2007. Identification and functional expression of the Arabidopsis thaliana vacuolar glucose transporter 1 and its role in seed germination and flowering. PNAS 104, 2537–2542.
Bais, H.P., Weir, T.L., Perry, L.G., Gilroy, S., Vivanco, J.M., 2006. The role of root exudates in rhizosphere interactions with plants and other organisms. Annu. Rev. Plant Biol. 57, 233–266.
Bermejo, C., Haerizadeh, F., Takanaga, H., Chermak, D., Frommer, W.B., 2010. Dynamic analysis of cytosolic glucose and ATP levels in yeast using optical sensors. Biochem. J. 432, 399–406.
Bessell, E.M., Thomas, P., 1973. The deoxyfluoro-D-glucopyranose 6-phosphates and their effect on yeast glucose phosphate isomerase. Biochem. J. 131, 77–82.
Biemelt, S., Sonnewald, U., 2006. Plant-microbe interactions to probe regulation of plant carbon metabolism. J. Plant Physiol. 163, 307–318.
Chaudhuri, B., Hormann, F., Lalonde, S., Brady, S.M., Orlando, D.A., Benfey, P., Frommer, W.B., 2008. Protonophore- and pH-insensitive glucose and sucrose accumulation detected by FRET nanosensors in Arabidopsis root tips. Plant J. 56, 948–962.
Chaudhuri, B., Hormann, F., Frommer, W.B., 2011. Dynamic imaging of glucose flux impedance using FRET sensors in wild-type Arabidopsis plants. J. Exp. Bot. 62, 2411–2417.
Chen, L.Q., Hou, B.H., Lalonde, S., Takanaga, H., Hartung, M.L., Qu, X.Q., Guo, W.J., Kim, J.G., Underwood, W., Chaudhuri, B., Chermak, D., Antony, G., White, F.F., Somerville, S.C., Mudgett, M.B., Frommer, W.B., 2010. Sugar transporters for intercellular exchange and nutrition of pathogens. Nature 468, 527–532.
Chen, H.Y., Huh, J.H., Yu, Y.C., Ho, L.H., Chen, L.Q., Tholl, D., Frommer, W.B., Guo, W.J., 2015a. The Arabidopsis vacuolar sugar transporter SWEET2 limits carbon sequestration from roots and restricts Pythium infection. Plant J. 83, 1046–1058.
Chen, L.Q., Cheung, L.S., Feng, L., Tanner, W., Frommer, W.B., 2015b. Transport of sugars. Annu. Rev. Biochem. 84, 865–894.
Cho, Y.H., Yoo, S.D., Sheen, J., 2006. Regulatory functions of nuclear hexokinase1 complex in glucose signaling. Cell 127, 579–589.
Cho, J.I., Ryoo, N., Eom, J.S., Lee, D.W., Kim, H.B., Jeong, S.W., Lee, Y.H., Kwon, Y.K., Cho, M.H., Bhoo, S.H., Hahn, T.R., Park, Y.I., Hwang, I., Sheen, J., Jeon, J.S., 2009. Role of the rice hexokinases OsHXK5 and OsHXK6 as glucose sensors. Plant Physiol. 149, 745–759.
Coudert, Y., Perin, C., Courtois, B., Khong, N.G., Gantet, P., 2010. Genetic control of root development in rice, the model cereal. Trends Plant Sci. 15, 219–226.
Dentin, R., Pégorier, J.-P., Benhamed, F., Foufelle, F., Ferré, P., Fauveau, V., Magnuson, M.A., Girard, J., Postic, C., 2004. Hepatic glucokinase is required for the synergistic action of ChREBP and SREBP-1c on glycolytic and lipogenic gene expression. J. Biol. Chem. 279, 20314–20326.
Deuschle, K., Okumoto, S., Fehr, M., Looger, L.L., Kozhukh, L., Frommer, W.B., 2005. Construction and optimization of a family of genetically encoded metabolite sensors by semirational protein engineering. Protein Sci. 14, 2304–2314.
Deuschle, K., Chaudhuri, B., Okumoto, S., Lager, I., Lalonde, S., Frommer, W.B., 2006. Rapid metabolism of glucose detected with FRET glucose nanosensors in epidermal cells and intact roots of Arabidopsis RNA-silencing mutants. Plant Cell 18, 2314–2325.
Dodd, A.N., Kudla, J., Sanders, D., 2010. The language of calcium signaling. Annu. Rev. Plant Biol. 61, 593–620.

Edwards, S., Nguyen, B.-T., Do, B., Roberts, J.K.M., 1998. Contribution of malic enzyme, pyruvate kinase, phosphoenolpyruvate carboxylase, and the krebs cycle to respiration and biosynthesis and to intracellular pH regulation during hypoxia in maize root tips observed by nuclear magnetic resonance imaging and gas chromatography-mass spectrometry. Plant Physiol. 116, 1073–1081.
Ettenhuber, C., Spielbauer, G., Margl, L., Hannah, L.C., Gierl, A., Bacher, A., Genschel, U., Eisenreich, W., 2005. Changes in flux pattern of the central carbohydrate metabolism during kernel development in maize. Phytochemistry 66, 2632–2642.
Farré, E.M., Tiessen, A., Roessner, U., Geigenberger, P., Trethewey, R.N., Willmitzer, L., 2001. Analysis of the compartmentation of glycolytic intermediates, nucleotides, sugars, organic acids, amino acids, and sugar alcohols in potato tubers using a non-aqueous fractionation method. Plant Physiol. 127, 685–700.
Fehr, M., Lalonde, S., Lager, I., Wolff, M.W., Frommer, W.B., 2003. In vivo imaging of the dynamics of glucose uptake in the cytosol of COS-7 cells by fluorescent nanosensors. J. Biol. Chem. 278, 19127–19133.
Gargallo-Garriga, A., Sardans, J., Perez-Trujillo, M., Rivas-Ubach, A., Oravec, M., Vecerova, K., Urban, O., Jentsch, A., Kreyling, J., Beierkuhnlein, C., Parella, T., Penuelas, J., 2014. Opposite metabolic responses of shoots and roots to drought. Sci. Rep. 4, 6829.
Gatenby, R.A., Gawlinski, E.T., 2003. The glycolytic phenotype in carcinogenesis and tumour invasion: insights through mathematical models. Cancer Res. 63, 3847–3854.
Granot, D., David-Schwartz, R., Kelly, G., 2013. Hexose kinases and their role in sugar-sensing and plant development. Front. Plant Sci. 4, 44.
Grigston, J.C., Osuna, D., Scheible, W.-R., Liu, C., Stitt, M., Jones, A.M., 2008. D-Glucose sensing by a plasma membrane regulator of G signaling protein, AtRGS1. FEBS Lett. 582, 3577–3584.
Guan, Y.F., Huang, X.Y., Zhu, J., Gao, J.F., Zhang, H.X., Yang, Z.N., 2008. RUPTURED POLLEN GRAIN1, a member of the MtN3/saliva gene family, is crucial for exine pattern formation and cell integrity of microspores in Arabidopsis. Plant Physiol. 147, 852–863.
Heineke, D., Wildenberger, K., Sonnewald, U., Willmitzer, L., Heldt, H.W., 1994. Accumulation of hexoses in leaf vacuoles: studies with transgenic tobacco plants expressing yeast-derived invertase in the cytosol, vacuole or apoplasm. Planta 194, 29–33.
Johnston, M., Kim, J.H., 2005. Glucose as a hormone: receptor-mediated glucose sensing in the yeast Saccharomyces cerevisiae. Biochem. Soc. T. 33, 247–252.
Kim, Y.M., Heinzel, N., Giese, J.O., Koeber, J., Melzer, M., Rutten, T., Von Wiren, N., Sonnewald, U., Hajirezaei, M.R., 2013. A dual role of tobacco hexokinase 1 in primary metabolism and sugar sensing. Plant Cell Environ. 36, 1311–1327.
Kim, H.B., Cho, J.I., Ryoo, N., Shin, D.H., Park, Y.I., Hwang, Y.S., Lee, S.K., An, G., Jeon, J.S., 2016. Role of rice cytosolic hexokinase OsHXK7 in sugar signaling and metabolism. J. Integr. Plant Biol. 58, 127–135.
Lastdrager, J., Hanson, J., Smeekens, S., 2014. Sugar signals and the control of plant growth and development. J. Exp. Bot. 65, 799–807.
Lin, W., Schmitt, M.R., Hitz, W.D., Giaquinta, R.T., 1984. Sugar-transport into protoplasts isolated from developing soybean cotyledons .1. Protoplast isolation and general-characteristics of sugar-transport. Plant Physiol. 75, 936–940.
Ma, G., Wei, M., He, L., Liu, C., Wu, B., Zhang, S.L., Jing, J., Liang, X., Senes, A., Tan, P., Li, S., Sun, A., Bi, Y., Zhong, L., Si, H., Shen, Y., Li, M., Lee, M.S., Zhou, W., Wang, J., Wang, Y., Zhou, Y., 2015. Inside-out Ca(2 +) signalling prompted by STIM1 conformational switch. Nature Commun. 6, 7826.
Moore, B., Zhou, L., Rolland, F., Hall, Q., Cheng, W.H., Liu, Y.X., Hwang, I., Jones, T., Sheen, J., 2003. Role of the Arabidopsis glucose sensor HXK1 in nutrient, light, and hormonal signaling. Science 300, 332.
Moreno, F., Ahuatzi, D., Riera, A., Palomino, C.A., Herrero, P., 2005. Glucose sensing through the Hxk2-dependent signalling pathway. Biochem. Soc. T. 33, 265–268.
Rolland, F., Baena-Gonzalez, E., Sheen, J., 2006. Sugar sensing and signaling in plants: conserved and novel mechanisms. Annu. Rev. Plant Biol. 57, 675–709.
Servaites, J.C., Geiger, D.R., 2002. Kinetic characteristics of chloroplast glucose transport. J. Exp. Bot. 53, 1581–1591.
Shah, N.H., Paulsen, G.M., 2003. Interaction of drought and high temperature on photosynthesis and grain-filling of wheat. Plant Soil 257, 219–226.
Shavrukov, Y., 2013. Salt stress or salt shock: which genes are we studying? J. Exp. Bot. 64, 119–127.
Smeekens, S., Hellmann, H.A., 2014. Sugar sensing and signaling in plants. Front. Plant Sci. 5, 113.
Steinhorst, L., Kudla, J., 2014. Signaling in cells and organisms − calcium holds the line. Curr. Opin. Plant Biol. 22, 14–21.
Turhan, E., Ergin, S., 2012. Soluble sugars and sucrose-metabolizing enzymes related to cold acclimation of sweet cherry cultivars grafted on different rootstocks. Scientific World J. 2012, 979682.
Wang, Z., Chen, C., Xu, Y., Jiang, R., Han, Y., Xu, Z., Chong, K., 2004. A practical vector for efficient knockdown of gene expression in rice (Oryza sativa L.). Plant Mol. Biol. Rep. 22, 409–417.
Xiong, Y., McCormack, M., Li, L., Hall, Q., Xiang, C., Sheen, J., 2013. Glucose-TOR signalling reprograms the transcriptome and activates meristems. Nature 496, 181–186.
Yoshida, S., Forno, D.A., Cock, J.H., Gomez, K.A., 1976. Routine Procedure for Growing Rice Plants in Culture Solution. Laboratory Manual for Physiological Studies of Rice, third edition. IRRI, Los Banos (Chapter 17).
Zhang, Y., Wang, Y., Taylor, J.L., Jiang, Z., Zhang, S., Mei, F., Wu, Y., Wu, P., Ni, J., 2015. Aequorin-based luminescence imaging reveals differential calcium signalling responses to salt and reactive oxygen species in rice roots. J. Exp. Bot. 66, 2535–2545.
Zhou, J., Peng, Z., Long, J., Sosso, D., Liu, B., Eom, J.S., Huang, S., Liu, S., Vera Cruz, C., Frommer, W.B., White, F.F., Yang, B., 2015. Gene targeting by the TAL effector PthXo2 reveals cryptic resistance gene for bacterial blight of rice. Plant J. 82, 632–643.